A&A 536, A68 (2011)
DOI: 10.1051/0004-6361/201117549

Astronomy & Astrophysics

Slow magnetacoustic waves in magnetic arcades

M. Gruszecki[1] and V. M. Nakariakov[1,2]

[1] Centre for Fusion, Space and Astrophysics, Department of Physics, University of Warwick, Coventry CV4 7AL, UK
e-mail: M.Gruszecki@warwick.ac.uk
[2] Central Astronomical Observatory at Pulkovo of the Russian Academy of Sciences, 196140 St Petersburg, Russia

Received 23 June 2011 / Accepted 21 October 2011

ABSTRACT

Aims. We investigate two-dimensional effects on the evolution of impulsively-generated slow magnetoacoustic waves in magnetic arcades of the solar corona.
Methods. We used a two-dimensional box model of a coronal arcade, neglecting the effects of gravity and magnetic curvature. Ideal finite-β magnetohydrodynamic equations were employed. The plasma was taken to be uniform, penetrated by a straight and uniform magnetic field. We applied line-tying boundary conditions at the magnetic footpoints.
Results. Running and standing slow magnetoacoustic waves develop across the magnetic field due to the reflection from the footpoints in the arcade. The perpendicular group speed is lower than both sound and Alfvén speeds. The speed grows with the increase in plasma-β, which is consistent with analytical theory. Slow magnetoacoustic pulse perturbs the magnetic field and current density; this effect is stronger for higher amplitudes. Standing waves spread across the field, forming a characteristic phase-mixing pattern of anti-parallel flows. The two-dimensional effects are more pronounced for higher β. Our results confirm the plausibility of the interpretation of the observed evolution of two-ribbon flares in terms of slow magnetoacoustic waves in magnetic arcades.

Key words. magnethydrodynamics (MHD) – Sun: corona

1. Introduction

Slow magnetoacoustic waves are one of the most studied magnetohydrodynamic (MHD) wave modes in the solar corona (see De Moortel 2006; Roberts 2006; De Moortel 2009, for recent reviews). Slow waves are detected in open and closed magnetic structures in the form of propagating (e.g. Verwichte et al. 2010) and standing (e.g. Wang 2011) waves. In a low-β plasma of the corona, slow magnetoacoustic waves propagate almost parallel to the magnetic field, and are mainly characterised by the perturbations of the plasma density and field-aligned flows. Because slow waves are essentially compressible, they are usually detected with imaging instruments as variations of the emission intensity, propagating along the presumed direction of the magnetic field (e.g. De Moortel et al. 2002). In some cases slow waves are also detected with spectral instruments that investigate the Doppler shift of coronal emission lines (e.g. Wang et al. 2003; Erdélyi & Taroyan 2008; Wang et al. 2009; Mariska & Muglach 2010; Van Doorsselaere et al. 2011). Typical periods of observed coronal slow waves are several minutes, and, in agreement with the MHD wave theory, the measured projected phase speed is typically subsonic.

The interest in coronal slow waves is primarily linked with their seismological potential. In particular, propagating slow waves were used for probing fine, sub-resolution structuring of active regions (King et al. 2003) by the apparent decrease in the correlation of the propagating disturbances seen in different EUV bandpasses. Coordinated imaging and spectral observations of standing slow waves led to the estimation of the magnetic field strength in the waveguiding loops (Wang et al. 2009). Recently, the spectroscopically measured phase lag between the temperature and density perturbations in propagating slow waves was used to estimate of the effective adiabatic index γ (Van Doorsselaere et al. 2011). In addition, the recently established phenomenological relationship between sunspot oscillations and quasi-periodic energy releases in solar flares (Sych et al. 2009), including slow waves as the signal carrier, opens up interesting perspectives for the seismological study of flaring sites and flare-triggering mechanisms. Very recently, Nakariakov & Zimovets (2011) demonstrated that slow magnetoacoustic waves could be responsible for the observed progression of flaring energy releases along a magnetic neutral line (and hence across the equilibrium magnetic field) in two-ribbon flares. It was shown that in coronal arcades slow magnetoacoustic waves propagate across a magnetic field at a group speed significantly lower than both the sound and Alfvén speeds, and that this behaviour was well-consistent with the observed evolution of two-ribbon flares. We aim to contribute to the understanding of this effect. In our numerical simulation we did not consider the whole "chain" of the physical processes leading to the progression of the flare along the arcade, including the "ignition" of magnetic reconnection by a slow pulse. Instead, we considered an individual act of the process, one of the two key building blocks of it: the "delivery" of the information about an energy release burst to another possible point of the release, at some distance along the axis of the arcade. We generalised the qualitative estimates of Nakariakov & Zimovets (2011) for broadband slow pulses of finite amplitude.

The traditional approach to the theoretical description of slow waves in the solar corona is a simple one-dimensional model, which restricts attention to the field-aligned motions only and allows one to study in detail effects of stratification, thermal conduction, viscosity, radiation, flux tube divergence

and nonlinearity (Ofman et al. 1999; Nakariakov et al. 2000; Ofman & Wang 2002; De Moortel & Hood 2004; Nakariakov et al. 2004; Taroyan et al. 2005; De Moortel & Bradshaw 2008; Taroyan & Bradshaw 2008). Essentially, this model reduces slow magnetoacoustic waves to acoustic waves, which dramatically simplifies the analysis. However, this approach excludes some important effects from the consideration, such as the perturbations of the magnetic field in the wave. The magnetic effects may be important, because they modify, e.g., the propagation speed of the slow wave guided by a magnetic flux tube. Indeed, the analysis of slow wave dispersion relations derived in the magnetic cylinder model (e.g. Edwin & Roberts 1983) shows that the propagating speed of slow waves is actually subsonic and is affected by the strength of the magnetic field. This dependence was, in particular, used for the magnetic field diagnostics by Roberts (2006) and Wang et al. (2009). The majority of two-dimensional studies of coronal slow waves (e.g. Selwa et al. 2007; Ogrodowczyk et al. 2009; Konkol et al. 2010) addressed the effects of stratification and magnetic field curvature, and hence were carried out in the plane perpendicular to the solar surface. On the other hand, the study of the slow wave progression in the direction perpendicular to the magnetic field in, e.g., two-ribbon flare arcades, requires their modelling in the plane parallel to the solar surface.

In this paper we present parametric numerical studies of oblique effects associated with slow magnetoacoustic waves in coronal arcades. Both running and standing waves are considered. We aim to develop the study of Nakariakov & Zimovets (2011) by accounting for the effects of broadband spectrum and nonlinearity. This paper is organised as follows. The analytical model and numerical methods are described in Sect. 2. Results of the simulations are presented and discussed in Sect. 3. We conclude with a summary of the main results in Sect. 4.

2. Numerical setup

2.1. Magnetohydrodynamic equations and numerical methods

We performed numerical simulations in a two-dimensional arcade filled in with a uniform plasma of constant temperature. We neglected gravity and non-adiabatic effects. Accordingly, we used the ideal magnetohydrodynamic equations to model the solar plasma:

$$\frac{\partial \varrho}{\partial t} + \nabla \cdot (\varrho \boldsymbol{V}) = 0, \tag{1}$$

$$\varrho \frac{\partial \boldsymbol{V}}{\partial t} + \varrho(\boldsymbol{V} \cdot \nabla)\boldsymbol{V} = -\nabla p + \frac{1}{\mu}(\nabla \times \boldsymbol{B}) \times \boldsymbol{B}, \tag{2}$$

$$\frac{\partial \boldsymbol{B}}{\partial t} = \nabla \times (\boldsymbol{V} \times \boldsymbol{B}), \tag{3}$$

$$\frac{\partial p}{\partial t} + \boldsymbol{V} \cdot \nabla p = -\gamma p \nabla \cdot \boldsymbol{V}, \tag{4}$$

$$\nabla \cdot \boldsymbol{B} = 0, \tag{5}$$

where ϱ is the mass density, p is the gas pressure, $\boldsymbol{B}$ is the magnetic field, $\boldsymbol{V}$ is the flow velocity, μ is the magnetic permeability and $\gamma = 5/3$ is the ratio of specific heats.

Equations (1–5) are numerically solved with the Lagrangian-remap code Lare2d (Arber et al. 2001). Lare2d operates by taking a Lagrangian predictor-corrector time step and after each Lagrangian step all variables are conservatively re-mapped back onto the original Eulerian grid using Van Leer gradient limiters. The code was designed for the simulation of nonlinear dynamics of low-β (the ratio of the gas pressure to the magnetic pressure) plasmas with steep gradients. In our studies we simulated the plasma dynamics in a domain $(-L, L) \times (-5L, 5L)$ where L is a half-width of the arcade, covered by 400×1000 grid points. We performed grid convergence studies to check the convergence of the numerical results.

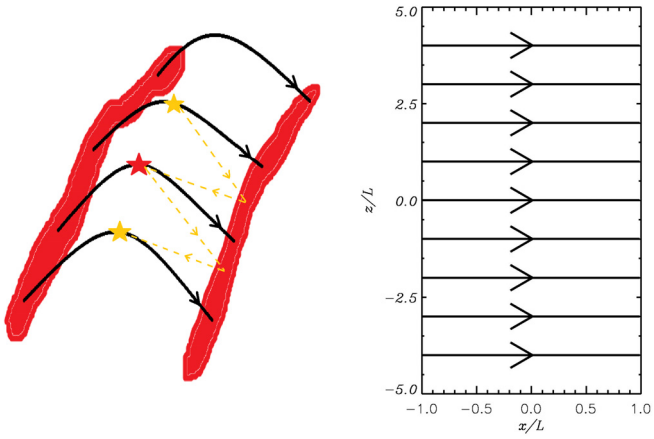

Fig. 1. Magnetic arcade of a two-ribbon flare (on the *left*) and its model (on the *right*) used during simulations. The black lines illustrate the magnetic field lines. The red regions in the left panel show the flare ribbons while we implemented line-tying boundary conditions at the left and the right boundary of simulation region. The yellow dashed lines show the race of the fastest slow magnetoacoustic waves. The red star shows the position of ignition of slow wave. The yellow stars show the positions of the secondary energy releases induced by the slow magnetoacoustic pulses.

2.2. The equilibrium and initial perturbation

We begin with an equilibrium that corresponds to a "box" model of a two-dimensional magnetic arcade (see Fig. 1). The arcade is considered as a sheet formed by the family of the magnetic field lines that link the ribbons of the arcade. Locally, the field lines are parallel to the sheet. In the model, the sheet is considered as a plane. The magnetic field is straight and uniform B_0 along x direction, and perpendicular to the arcade footpoints. We assumed that the length of the field lines was $2L$. The equilibrium plasma density ϱ and the plasma temperature T were taken to be constant everywhere. During the simulation we changed the value of plasma-β, choosing different values of sound speed c_s ranging from $0.5V_A$ to $0.8V_A$, where V_A is the Alfvén speed. We set line-tying boundary conditions along z direction at $x = \pm L$, while zero gradients were applied at the boundaries of the computational domain at $z = \pm 5L$.

We aimed to study impulsively excited slow waves in the simulation region. We considered the evolution of running and standing slow magnetoacoustic waves. To trigger a running wave we used an initial pulse in the temperature, localised somewhere in the arcade,

$$T(x, z) = T_a \exp\left[-\frac{(x - x_0)^2 + (z - z_0)^2}{w^2}\right] + T_0, \tag{6}$$

where T_0 is an equilibrium value of temperature, T_a is the amplitude of the initial pereturbation and w is its width. We chose two positions of the initial pulse: at the top $x_0/L = z_0/L = 0$ and at the footpoints $x_0/L = \pm 1$, $z_0/L = 0$, of the arcade, corresponding to the apex and footpoint heating, respectively. We also

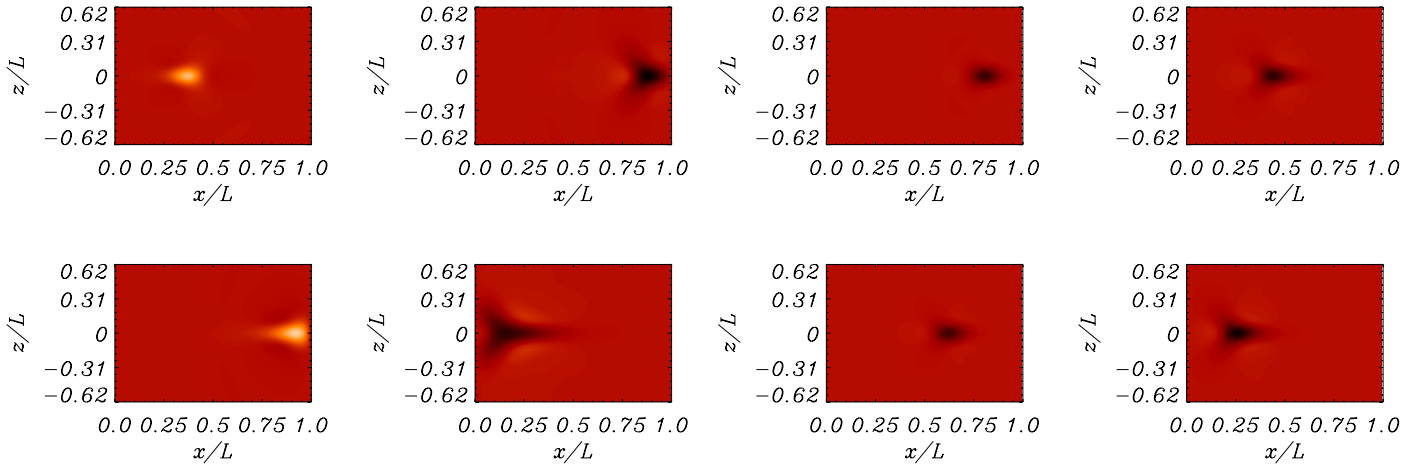

Fig. 2. Snapshots of the development of a slow magnetoacoustic pulse excited at the apex of a magnetic arcade for $\beta = 0.3$. The x-component of velocity, parallel to the equilibrium magnetic field, is shown at times $t = 15$ s (*top left panel*), $t = 37.5$ s, (*top right panel*) before the reflection from the footpoint, and at $t = 45$ s, (*bottom left panel*) and $t = 75$ s (*bottom right panel*) after the reflection. The pulse is excited by a localised increase in the plasma temperature given by Eq. (6), where $T_a = 0.1T_0$ and $w = 0.1$. The spatial coordinates are measured in units of L, which is the half width of the arcade. The panels show half of the computational domain, from the apex $x = 0$ to the footpoint $x = L$.

Fig. 3. Snapshots of the development of a slow magnetoacoustic pulse excited at the footpoint of a magnetic arcade for $\beta = 0.3$. The x component of velocity V_x is shown at times $t = 7.5$ s (*top left panel*), $t = 15$ s, (*top right panel*), $t = 22.5$ s, (*bottom left panel*) and $t = 30$ s (*bottom right panel*). To excite the slow wave, we used the same parameters for the initial pulse as in Fig. 2.

considered the evolution of a standing wave (e.g. Nakariakov et al. 2004), localised in the direction perpendicular to the field. We set the perturbation in the x (parallel to the field) component of the velocity:

$$V_x(x, z) = A_0 \sin(kx) \exp\left[-\frac{(z - z_0)^2}{w^2}\right], \quad (7)$$

where k is the wave number prescribed by the boundary conditions. In that part of our study, we restricted our attention to the excitation of second harmonic of the slow standing wave, with $k = 2\pi/L$. In our studies we demonstrated that the slow pulse (even of a finite amplitude) can indeed progress across the field, reaching the possible site of the next act of reconnection at a certain distance from the initial position along the arcade (Nakariakov & Zimovets 2011). The second "building block" of the model, triggering of the other act of magnetic reconnection by the slow wave, was not addressed in the present paper but our work is a very important step towards the full modelling of the whole chain of the processes involved.

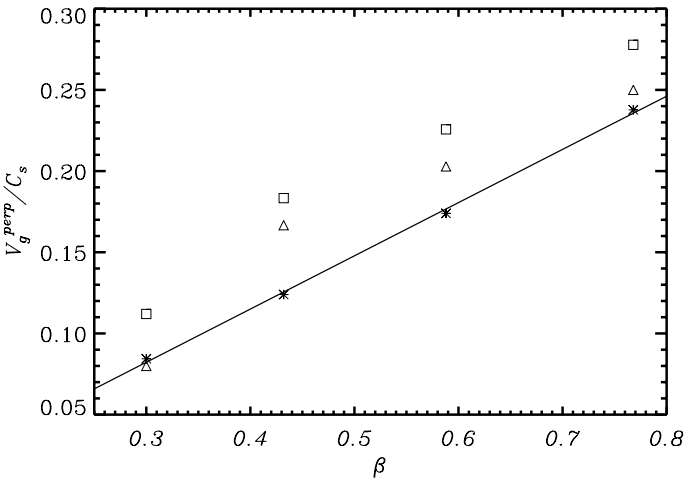

Fig. 4. Dependence of the perpendicular group speed of a slow magnetoacoustic pulse on the plasma-β. The stars correspond to the analytical estimate from the dispersion relation, while squares and triangles represent numerical results for $T_a = 0.1T_0$ and $T_a = 0.8T_0$, respectively. The analytically calculated points are fited with a linear function (the solid line).

3. Numerical results

3.1. Propagating pulses

Consider the development of a pulse with an increased temperature, initially localised in the arcade. After the excitation, the pulse splits into two slow magnetoacoustic pulses, which propagate mainly along the magnetic field in both directions, towards the footpoints. At the initial position remains a non-propagating entropy mode. A part of the energy also goes to the fast magnetoacoustic waves, propagating mainly across the field, in the directions parallel to the footpoints.

Figure 2 shows two-dimensional snapshots of the field-aligned velocity perturbations V_x, which represent the slow wave at different instants of time. The initial position of the pulse is at the arcade apex. The panels show only a half of the computational domain in the direction along the field to the right from the apex. Evidently, the slow pulse is reflected at the footpoint and returns to the apex. The direction of the parallel velocity perturbation changes the sign after the reflection. This propagation is accompanied by a gradual diffusion of the pulse across the magnetic field, and hence along the axis of the arcade. The initially Gaussian pulse gradually attains a "fork-like" shape. This scenario is consistent with the analytical results obtained in Nakariakov & Zimovets (2011). Indeed, the two-dimensional slow magnetoacoustic pulse evolves according to the dispersion relation: the highest perpendicular group speed is reached in the direction oblique to the magnetic field, hence the fork-like shape of the pulse. A pulse initially located at the footpoints of the arcade shows a very similar evolution (Fig. 3): the pulse, excited at $x = L$ propagates to the left, towards the apex, and gradually diffuses across the field, forming the fork-like structure.

According to the theory (see Fig. 3 of Nakariakov & Zimovets 2011), the perpendicular group speed grows with the

plasma-β. Figure 4 illustrates the dependence of the perpendicular group speed V_g^{perp} of a slow pulse upon the plasma parameter β. The speed was estimated as the ratio of the distance between the edge, defined by width of the initial pulse, and the point on the $z = 0$ line that the "prong" of the reflected pulse reaches first, to the travel time. We compared the numerical results with the perpendicular group speed obtained from the slow wave dispersion relation (Goedbloed & Poedts 2004):

$$\omega^2 = 0.5[(c_A^2 + c_s^2)(k_x^2 + k_z^2) - \sqrt{(c_A^2 + c_s^2)(k_x^2 + k_z^2)^2 - 4c_s^2 c_A^2 k_x^2 (k_x^2 + k_z^2)}], \quad (8)$$

where ω, k_x and k_z are the angular frequency, and the parallel and perpendicular wave numbers, respectively, and c_A and c_s are the Alfvén and sound speeds. The perpendicular group speed $V_g^{perp} = d\omega/dk_z$ calculated for $k_x = 2\pi/L$ is shown in the figure, too. The analytical estimation is qualitatively consistent with the numerical results. The quantitative discrepancy can be attributed to the difficulties in comparing essentially broadband numerical results with essentially monochromatic analytical estimation. The problem is connected with the ambiguity in the definition of the wave travel distance. Depending on what are taken as the initial and the end positions of the pulse (e.g. the centres of weight, leading and/or trailing slopes, etc.), the travel distance and hence the apparent speed are different. However, qualitatively the results should be consistent with the values given by dispersion relation. The discrepancy also will decrease with the increase in the travel distance.

Clearly, a compressible pulse should excite both slow and fast magnetoacoustic waves. The slow wave propagates mainly along the field, while the fast one does it mainly across the field. The relative strength of the excited magnetoacoustic pulses is determined by the excitation conditions. In our study, the localised pulse of the increase in the temperature is seen to result mainly in the slow wave. However, the fast wave is excited, too. Figure 5 illustrates profiles of $V_x^2 + V_z^2$, which are associated with the fast and slow waves, at $t = 17.5$ s after the impulsive excitation. The fast pulses form the horseshoe-like structures, propagating across the field and obliquely to it, while the slow waves have the fork-like shape discussed above. In addition, the fast and slow pulses propagate at different speed. Therefore, we can easily distinguish between these two magnetoacoustic waves in our study. The ratio of the maximum amplitudes of the velocity perturbations in the slow and fast waves is shown in Fig. 6. The amplitude of the fast wave is about an order of magnitude weaker than the amplitude of the slow wave. The relative amplitude of the fast wave grows with plasma-β. But, according to Fig. 5, the area occupied by the fast wave is much larger than the area of the slow wave. To estimate the partition of the energy in the waves, we calculated the integrals:

$$E = \int_S \int \left(V_x^2 + V_z^2\right) dx dz, \quad (9)$$

over the regions S, occupied by the waves. The regions of integration are shown in Fig. 5. It is seen in Fig. 6 that the fraction of the energy going to the fast wave is several times lower than the fraction of the energy going to the slow wave. Like the amplitude ratio, the energy ratio grows with plasma-β. This partition of energy is a feature of the specific method of the wave excitation. One can readily change this partition by exciting the waves by, e.g., a pulse of a perpendicular velocity or the magnetic field perturbation (see, e.g. Van Doorsselaere et al. 2008). However, a detailed investigation of those scenarios is out of scope of this study.

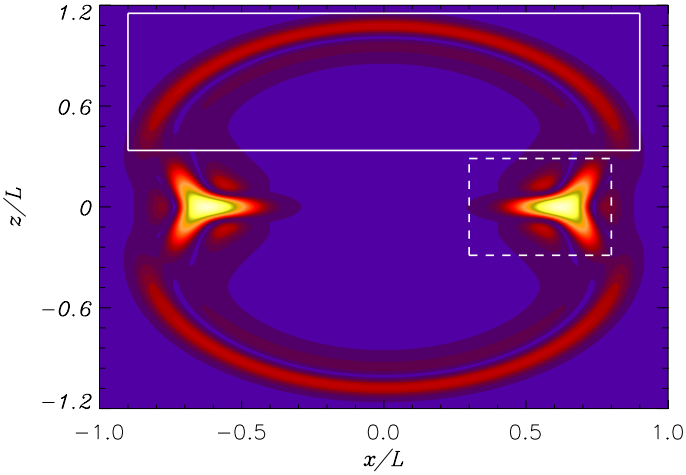

Fig. 5. Snapshot of the perturbation of $V_x^2 + V_z^2$ at $t = 17.5$ s, excited by a temperature pulse for $T_a = 0.1T_0$ located at top of the arcade. The boxes show the regions occupied by the fast (solid line) and the slow (dashed line) pulses, propagating in the positive directions of the z- and x-axis, respectively.

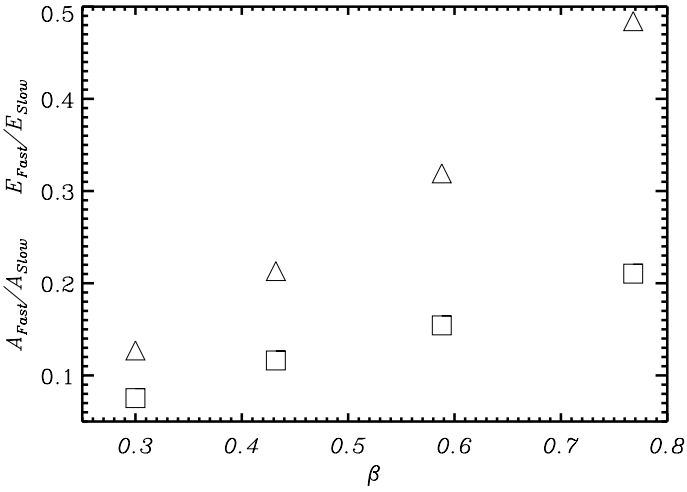

Fig. 6. Ratio of kinetic energy (triangles) and maximum velocity perturbations $\sqrt{V_x^2 + V_z^2}$ (squares) in the excited fast and slow magnetoacoustic waves as a function of plasma-β. The results were obtained for $T_a = 0.1T_0$.

In contrast to the acoustic wave, in a plasma with finite β slow magnetoacoustic waves perturb not only the plasma density ϱ, temperature and the parallel component of the plasma velocity V_x, but also the perpendicular components of the velocity, and the magnetic field B. The latter is also associated with the current density j.

Figure 7 shows snapshots of the mass density ϱ, the x component of velocity V_x (parallel to the field), the absolute value of the magnetic field $|B|$ and the current density j_y (this component of the current density is perpendicular to the plane of the simulation), at time $t = 50$ s. The snapshots are shown after the reflection, when the pulse returns back to the arcade apex. In the figure the pulse propagates from right to left. The fork-like structure is seen in all these physical quantities, hence it first reaches the apex not at the point of the excitation, but at some distance, which is determined by the perpendicular component of the group speed. We demonstrated that there is a build-up of the electric current density in the slow pulse, which can be responsible for the onset of current-driven plasma instabilities and

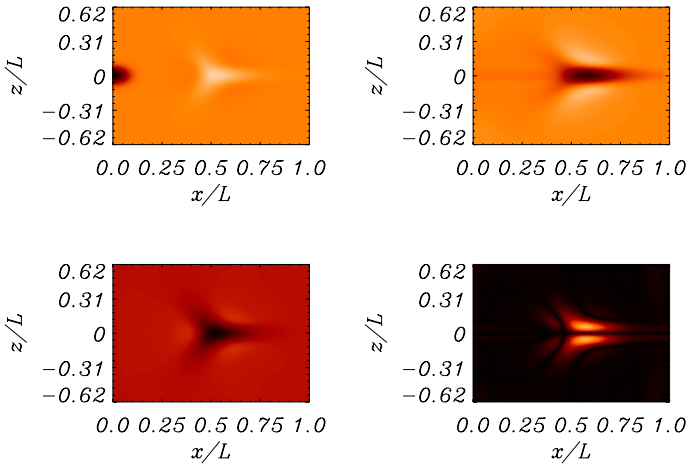

Fig. 7. Snapshots of the perturbations of the mass density ϱ (*top left panel*), the parallel component of the velocity (*top right panel*), the absolute value of the magnetic field $|B|$ (*bottom left panel*) and the current density j (*bottom right panel*) in a propagating slow magnetoacoustic pulse. The pulse is shown at the time $t = 67.5$ s, after the reflection from the arcade footpoint. The results were obtained for $T_a = 0.1T_0$.

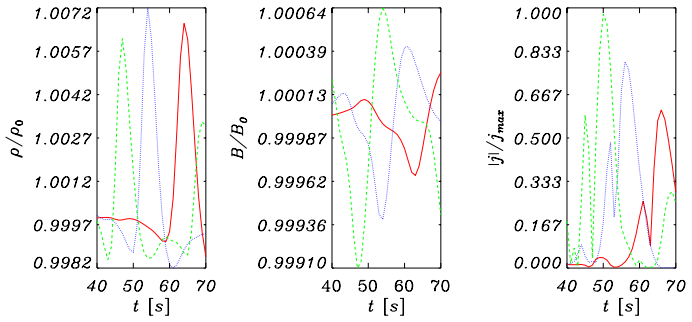

Fig. 8. Time profiles of the perturbations of mass density, magnetic induction and current density in a slow magnetoacoustic pulse, measured at $x/L = 0.1$ and $z/L = 0.05$ for different values of plasma β. The initial shape of the pulse is Gaussian. The solid (red) curve corresponds to $\beta = 0.3$, dotted (blue) $\beta = 0.43$ and dashed (green) $\beta = 0.59$. The results were obtained for $T_a = 0.1T_0$.

hence the anomalous resistivity. Thus the impulsively excited slow magnetoacoustic pulse can trigger another act of magnetic reconnection and set up the next part of the chain of the process proposed by Nakariakov & Zimovets (2011). The repetition of this cycle is supposed to explain the observed post-flare arcade. However, we stress that in our work we did not model the whole chain of the processes.

Figures 8, 9 show a typical shape of the perturbations of physical quantities in a slow magnetoacoustic pulse. Figure 8 illustrates the time profiles of the perturbed quantities for different values of plasma-β. The perturbations of the mass density ϱ, the absolute value of the magnetic field $|B|$ and the current density j are measured in the vicinity of the apex, at the point $(x/L = 0.1, z/L = 0.1)$. The measurements were made before the collision with the pulse, reflected from the opposite footpoint, and approaching the apex from the opposite direction. The value of j_{max} corresponds to the maximum current density obtained for $\beta = 0.59$. Evidently, the slow magnetoacoustic waves propagate faster and have a more pronounced "magnetic" component for the higher value of β. Figure 9 shows similar time profiles, but for different initial amplitudes. The shape of slow pulses of higher amplitude experiences nonlinear steepening, and have stronger perturbations of the current density.

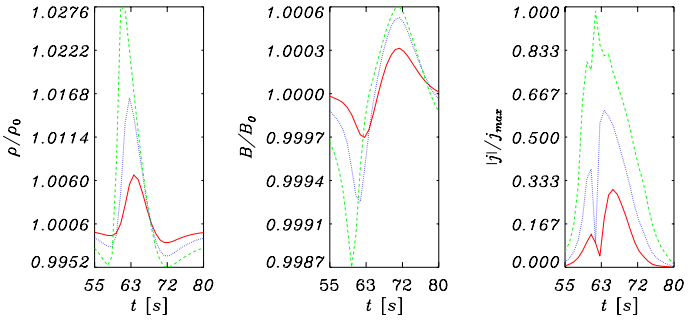

Fig. 9. Similar to Fig. 8, but for different amplitudes of the initial pulse: red (solid) line $T_a = 0.1T_0$, blue (dotted) line $T_a = 0.25T_0$ and green (dashed) line $T_a = 0.5T_0$.

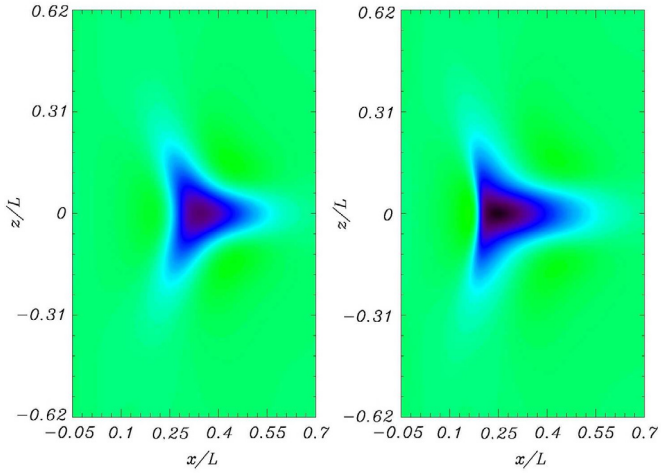

Fig. 10. Snapshots of the parallel component of the velocity in a slow magnetoacoustic pulse for two different amplitudes of initial perturbation: $T_a = 0.1T_0$ (*left panel*) and $T_a = 0.6T_0$ (*right panel*). The snapshots were taken at $t = 67.5$ s, after the reflection of the pulse from the right boundary, when the pulse was propagating to the left.

Figure 10 shows the effect of a finite amplitude on the two-dimentional shape of the slow magnetoacoustic pulse. Snapshots of the x-component of the velocity, taken at $t = 67.5$ s for two different amplitudes of the initial perturbation, $T_a = 0.1T_0$ (left panel) and $T_a = 0.6T_0$ (right panel) demonstrate that the fork-like shape of the pulse of the higher amplitude tends to be more triangular. The higher amplitude pulse is also wider in the transverse direction, across the field.

3.2. Standing wave

Consider standing slow magnetoacoustic waves in a flaring arcade, excited by a harmonic profile of the parallel velocity V_x (see Fig. 11, top left panel). Such a perturbation corresponds to the second spatial harmonics, which can be easily excited in a one-dimensional model by a localised deposition of, e.g., plasma heating (see, e.g. Tsiklauri et al. 2004). Initially, the perturbation has a localised Gaussian shape in the perpendicular direction.

Figure 11 display the evolution of the parallel velocity, mass density and current density in an initially localised standing slow wave in the transverse direction. The standing perturbation gradually progresses in the transverse direction, across the field, forming an oscillatory structure. The flows quickly become anti-parallel, forming a typical phase-mixing pattern. Current density

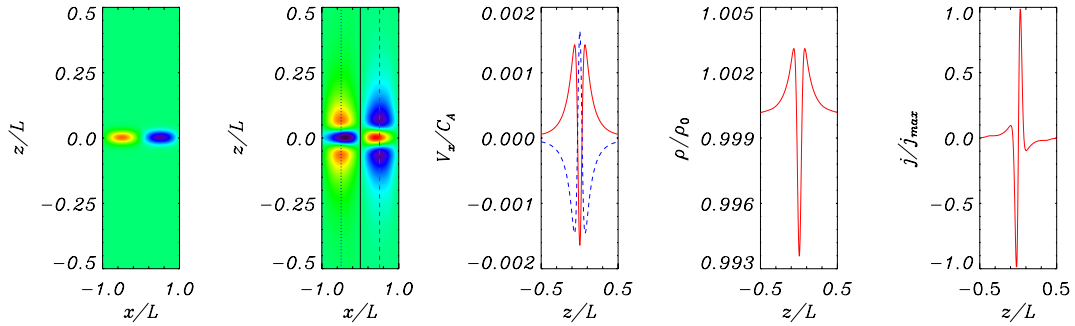

Fig. 11. Evolution of a standing slow magnetoacoustic wave at an arcade. *First panel*: contour plots of the parallel velocity along the magnetic field at the time $t = 0$. *Second panel*: contour plots of the parallel velocity at the time $t = 1.75P$, where P is the period of the oscillation. *Third panel*: transverse structure of the parallel velocity perturbation at $x/L = -0.75L$ (blue dotted line in second panel) at $t = 1.75P$ (red solid line) and $x/L = 0.75L$ (red line in second panel) at $t = 0.75P$ (blue dotted line). *Fourth panel*: transverse structure of the plasma density perturbation at the apex of the arcade (black solid line in the second panel) at $t = 2.0P$. *Fifth bottom panel*: transverse structure of the current density perturbation at the apex of the arcade (black solid line in the second panel) at $t = 2.0P$. The parameters of the pulse are $A_0 = 0.15V_A$, $w = 0.1\ L$ and $z_0 = 0$.

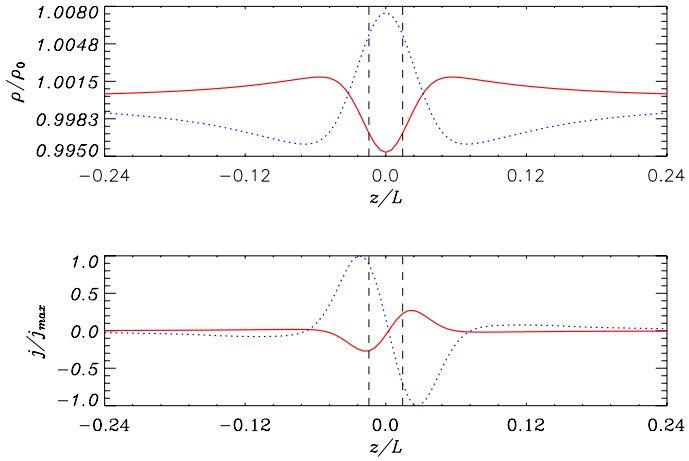

Fig. 12. Transverse profiles of the mass density (*top panel*) and current density (*bottom panel*) in a standing slow wave after two periods of oscillations. The red (solid) line corresponds to the case with $\beta = 0.3$, and the blue (dotted) line to $\beta = 0.76$. The dashed black lines show the initial half-width of the pulse.

spikes are generated in the regions of the steep gradients of the mass density. Thus, the 2D effects, associated with the perturbation of the magnetic field, can occur to be non-negligible and should be taken into account in the consideration of their dissipation and observational manifestation.

Similar to the case of a propagating wave, the relative strength of the magnetic component in the standing slow wave is determined by the plasma-β. Figure 12 illustrates this effect by showing the transverse profiles of the mass density and the current density perturbations in the wave for two different values of plasma β. For a higher value of β the perturbations have a broader extent across the field.

4. Summary and discussion

We performed a parametric study of running and standing broadband slow magnetoacoustic pulses in a magnetic arcade in frames of ideal MHD. The arcade was modelled as a box filled in with a uniform low-β plasma, penetrated by a constant and straight magnetic field. At the boundaries of the box across the field line-tying conditions were applied.

A slow magnetoacoustic pulse, excited by a localised increase in the plasma temperature, propagates in both directions along the magnetic field, and gradually develops in the direction across the field. The shape of the pulse becomes "fork-like", with obliquely extended prongs. The pulse shape is not destroyed by the reflection from the arcade footpoints. The speed of the propagation across the field is sub-sonic and sub-Alfvénic, growing with the increase in plasma-β. This scenario is independent of the position of the initial excitation. The speed of the progression across the field was found to be qualitatively consistent with the value obtained with analytical dispersion relations. Quantitatively, the comparison being complicated with the ambiguity is the definition of the pulse travel distance.

A slow magnetoacoustic pulse contains perturbations of the magnetic field and the current density. The "magnetic component" of the pulse grows with the increasing β. This component has usually been ignored in the theoretical studies of slow magnetoacoustic waves in the corona, when the waves were considered in their degenerated, purely acoustic form (e.g. Nakariakov et al. 2000, 2004; Ofman & Wang 2002; De Moortel & Hood 2004; De Moortel & Bradshaw 2008; Tsiklauri et al. 2004; Taroyan et al. 2005; Taroyan & Bradshaw 2008). Our results demonstrate that the magnetic component is an important part of a localised, non-plane slow magnetoacoustic perturbation and hence it should be taken into account in more rigorous studies.

Pulses of higher amplitude propagate faster in the parallel and perpendicular direction and are subject to nonlinear steepening and associated increase in the current density.

A spatially localised perturbation of plasma temperature excites slow and fast magnetoacoustic waves. Amplitude and energy of the excited fast wave are several times weaker than those of the slow waves.

Slow magnetoacoustic standing waves are also found to be subject to the progression across the field and development of the "magnetic component" – the perturbations of the magnetic field and the current density, more pronounced for higher β. Moreover, the progression across the field is accompanied by the generation of a phase-mixing pattern of anti-parallel field-aligned flows. Possible implications of this effect on the dissipation of the waves have been discussed in De Moortel et al. (2004); Voitenko et al. (2005). However, in contrast with those works, in our study phase-mixing appears in a medium, uniform in the direction across the field. The formation of contour flows

can also have interesting consequences in the manifestation of standing slow magnetoacoustic waves in spectral observations.

The evolution of a slow magnetoacoustic pulse was found to be well consistent with the model of the two-ribbon flare evolution (Nakariakov & Zimovets 2011). Moreover, our study demonstrates that the pulse could trigger another act of magnetic reconnection through the perturbation of the plasma density and the current density, the mechanisms developed in Chen & Priest (2006) and Nakariakov et al. (2006) for the generation of quasi-periodic pulsations observed in solar flares. However, the second "building block" of the model, triggering of the other act of magnetic reconnection by the slow wave, was not addressed in the present paper. We merely showed that a broadband slow magnetoacoustic pulse can perform the transfer of energy and information required for triggering the next energy release, across the magnetic field at the group speed consistent with the observed value.

Thus, two-dimensional effects on slow magnetoacoustic waves are found to be important and hence should be taken into account in the development of advanced low-dimensional models of propagating and standing coronal magnetoacoustic waves, especially in hot flaring plasmas.

Acknowledgements. M.G. is supported by the Newton International Fellowship NF090143.

References

Arber, T. D., Longbottom, A. W., Gerrard, C. L., & Milne, A. M. 2001, J. Comput. Phys., 171, 151
Chen, P. F., & Priest, E. R. 2006, Sol. Phys., 238, 313
De Moortel, I. 2006, Roy. Soc. London Philos. Trans. Ser. A, 364, 461
De Moortel, I. 2009, Space Sci. Rev., 149, 65
De Moortel, I., & Bradshaw, S. J. 2008, Sol. Phys., 252, 101
De Moortel, I., & Hood, A. W. 2004, A&A, 415, 705
De Moortel, I., Hood, A. W., Ireland, J., & Walsh, R. W. 2002, Sol. Phys., 209, 89
De Moortel, I., Hood, A. W., Gerrard, C. L., & Brooks, S. J. 2004, A&A, 425, 741
Edwin, P. M., & Roberts, B. 1983, Sol. Phys., 88, 179
Erdélyi, R., & Taroyan, Y. 2008, A&A, 489, L49
Goedbloed, J., & Poedts, S. 2004, Principles of Magnetohydrodynamics
King, D. B., Nakariakov, V. M., Deluca, E. E., Golub, L., & McClements, K. G. 2003, A&A, 404, L1
Konkol, P., Murawski, K., Lee, D., & Weide, K. 2010, A&A, 521, A34
Mariska, J. T., & Muglach, K. 2010, ApJ, 713, 573
Nakariakov, V. M., & Zimovets, I. V. 2011, ApJ, 730, L27
Nakariakov, V. M., Verwichte, E., Berghmans, D., & Robbrecht, E. 2000, A&A, 362, 1151
Nakariakov, V. M., Tsiklauri, D., Kelly, A., Arber, T. D., & Aschwanden, M. J. 2004, A&A, 414, L25
Nakariakov, V. M., Foullon, C., Verwichte, E., & Young, N. P. 2006, A&A, 452, 343
Ofman, L., & Wang, T. J. 2002, ApJ, 580, L85
Ofman, L., Nakariakov, V. M., & Deforest, C. E. 1999, ApJ, 514, 441
Ogrodowczyk, R., Murawski, K., & Solanki, S. K. 2009, A&A, 495, 313
Roberts, B. 2006, Roy. Soc. London Philos. Trans. Ser. A, 364, 447
Selwa, M., Ofman, L., & Murawski, K. 2007, ApJ, 668, L83
Sych, R., Nakariakov, V. M., Karlicky, M., & Anfinogentov, S. 2009, A&A, 505, 791
Taroyan, Y., & Bradshaw, S. 2008, A&A, 481, 247
Taroyan, Y., Erdélyi, R., Doyle, J. G., & Bradshaw, S. J. 2005, A&A, 438, 713
Tsiklauri, D., Nakariakov, V. M., Arber, T. D., & Aschwanden, M. J. 2004, A&A, 422, 351
Van Doorsselaere, T., Brady, C. S., Verwichte, E., & Nakariakov, V. M. 2008, A&A, 491, L9
Van Doorsselaere, T., Wardle, N., Del Zanna, G., et al. 2011, ApJ, 727, L32
Verwichte, E., Marsh, M., Foullon, C., et al. 2010, ApJ, 724, L194
Voitenko, Y., Andries, J., Copil, P. D., & Goossens, M. 2005, A&A, 437, L47
Wang, T. J. 2011, Space Sci. Rev., 158, 397
Wang, T. J., Solanki, S. K., Curdt, W., et al. B. 2003, A&A, 406, 1105
Wang, T. J., Ofman, L., & Davila, J. M. 2009, ApJ, 696, 1448